Received Date : 14-Jan-2011
Revised Date : 30-May-2011
Accepted Date : 17-Jun-2011
Article type : Original Article

T3 administration ameliorates the demyelination/remyelination ratio in a non-human primate model of multiple sclerosis by correcting tissue hypothyroidism.

G. D'Intino[2#], L. Lorenzini[2#], M. Fernandez[1], A. Taglioni[3], G. Perretta[3], G. Del Vecchio[2], P. Villoslada[4], L. Giardino[1], [*]L. Calzà[1]

[1]CIRI Life Sciences and Healt Technology and [2]Dep. of Veterinary Medicine, University of Bologna, Italy; [2]Institute of Neurobiology and Molecular Medicine, CNR, Roma; [3]Institut d'Investigacions Biomèdiques August Pi I Sunyer (IDIBAPS), Hospital Clinic, Barcelona, Spain

 # These authors contributed equally to the study

correspondence to:
Laura Calzà, MD
CIRI Life Sciences and Health Technologies, University of Bologna
Via Tolara di Sopra 50
I-40064 Ozzano Emilia (Bologna), Italy
Email laura.calza@unibo.it

Short title: **T3 ameliorates course of EAE in the marmoset**

Key words:
thyroid hormone; marmoset; remyelination; oligodendrocyte precursor cells; experimental allergic encephalomyelitis

Abstract

Remyelination failure is a key landmark in chronic progression of multiple sclerosis (MS), the most diffuse demyelinating disease in human, but the reasons for this are still unknown. It has been proved that thyroid hormone administration in the rodent models of acute and chronic demyelinating diseases improved their clinical course, pathology and remyelination. In this study we translated this therapeutic attempt to experimental allergic encephalomyelitis (EAE) in the non-human primate *Callithrix Jacchus* (*C. Jacchus*, marmoset). We report that short protocols of T3 treatment shifts the demyelination/remyelination balance toward remyelination, as assessed by morphology, immunohistochemistry and molecular biology, and improves the clinical course of the disease. We also found that severely ill animals display hypothyroidism and severe alteration of deiodinase and thyroid hormone receptor mRNAs expression in the spinal cord, which was completely corrected by thyroid hormone treatment. We therefore suggest that thyroid hormone treatment improves myelin sheath morphology in marmoset EAE, by correcting the dysfunction of thyroid hormone cellular effectors.

Introduction

Multiple sclerosis (MS) is an inflammatory-autoimmune disease of the central nervous system (CNS) lasting decades. The pathology of the disease includes inflammation, blood brain barrier disruption, autoimmune attack, demyelination and neurodegeneration (1). The acute, focal phase of the disease is characterized by inflammation and acute damage of the myelin sheath and axons. At this stage, remyelination may be robust and efficient and early lesions of the white matter (fresh plaques) may be completely and correctly repaired and function restored. This capability is largely guaranteed by the presence of a cell population in the CNS, which is identified by the presence of the membrane-associated chondroitin sulfate proteoglycan NG2 (NG2) and the α receptor for platelet-derived growth factor (PDGFαR). These cells, which were originally identified as oligodendrocyte precursor cells (OPCs) are disseminated within the white and grey matter of the adult CNS, accounting for 5-8 % of the total cell population, are activated in the case of injury, and are usually able to proliferate and differentiate into mature myelinating oligodendrocytes (2). For unknown reasons, this process

progressively fails in MS, in spite of the fact that a significant number of OPCs also newly generated from neural stem cells (NSCs) (3) are found in early lesions in MS (4). Actually, a blockage of OPCs is regarded as a preeminent cause of remyelination failure in MS (5). The progressive failure of remyelination leads to the cumulative loss of axons and prevalent neurodegeneration, which accounts for chronic disability and cognitive decline. Currently, remyelination failure is considered a frustrating feature in MS, a key event in triggering neurodegeneration and a reliable target for therapy also aimed to axonal protection (6).

As there are differences between the two processes, it is considered that successful remyelination recapitulates most of the molecular and cellular processes of developmental myelination (7). Evidence accumulated over the last decades proved that developmental myelination is a thyroid hormone- (TH) dependent process (8-10). In particular, studies in genetically modified animals (11), such as in hypo- and hyperthyroid animals (12), have provided abundant evidence that TH plays an important part in regulating oligodendrocyte lineage and maturation *in vivo*. THs induce more oligodendrocytes to form from multipotent neural stem cells and regulate several stages of oligodendrocyte development and maturation (13-15). Starting form this rationale, three independent laboratories, including ours, have proved that TH administration improves remyelination process and clinical course in acute and chronic demyelination models in rodents, favoring neuroprotection. Our work in experimental allergic encephalomyelitis (EAE) developed in Lewis and Dark-Agouti rats demonstrated that in vivo TH administration activates OPCs by promoting their maturation, protects myelin sheat and axons and finally improves clinical outcome (14,16-19). Moreover, T3 restores the oligodendroglial lineage and oligodendrocyte maturation from neural progenitors, which are lost in EAE (15,17,20). Other authors indicated that T3 administration improves remyelination in chronic demyelination models. Franco et al. (21) showed that remyelination in the corpus callosum of cuprizone-treated rats improved markedly when treated with T3, compared to saline-treated animals. Moreover, OLs decrease and OPCs increase in the SVZ, such as the inhibition of Olig and Shh expression observed in demyelinated animals were reversed after T3 administration, suggesting that THs could regulate the emergence of remyelinating OLs from the pool of proliferating cells. Harsan et al. (22) analyzed T3 effect on cuprizone demyelination in mice, using a combination of in vivo diffusion tensor magnetic resonance imaging (DT-MRI) and histological analyses. T3 restored the normal DT-MRI phenotype accompanied by an improvement of clinical signs

and remyelination. T3 also increased the expression of Shh and the number of *Olig2*- and PSA-NCAM-positive precursors and proliferative cells.

Starting from the above, we have explored the possibility of promoting myelination and/or protecting myelin sheath in EAE induced in the non-human primate *C. Jacchus* (marmoset) through the administration of TH. We also explored possible disease-associated mechanisms supporting TH effectiveness in EAE.

Materials and Methods

Animals, enrolling and group definition

The *C. Jacchus* used in this study were colony-born individuals and were maintained and utilised at the Italian National Research Council (CNR) Breeding Center in Rome. The animals were housed in extended family groups of 4 to 6 individuals consisting of a breeding pair and their offspring. Small groups of animals including two to four pairs were enrolled in each section of the study until a statistically significant difference was found in the clinical score between EAE placebo and EAE treated animals. Half of the pairs were immunized in each section of the enrolling phase, and immunized animals were treated either with thyroid hormone or with saline. The code record of enrolled animals was blind to the operators engaged in the immunization, treatments, animal scoring, tissue handling and processing; the code was clear for the study director, who was not directly involved in the animal experiments or in laboratory activities. The half-blind strategy was chosen in order to stop animals being enrolling as soon as experimental treatments produced statistically significant clinical effects. Immunization and sacrifice were performed under anaesthesia with 10 mg/kg of ketamine hydrochloride i.m. The experiments were carried out in accordance with current European and Italian legislations, and received the prior approval of the Italian Ministry of Health (Authorization n° 57/2004-C; extension DGVSA/10/n°18350). For morphological studies, N=4 animals were included in each group; for molecular studies, N=4 animals were included in the control group and N=6 were included in both EAE and EAE+T3 groups (see Table I).

Immunization protocol, thyroid hormone treatments and clinical features of EAE

The immunogenic solution used for this study was composed of the peptide human recombinant MOG corresponding to the N-terminal part of human MOG (1-125; hrMOG) (23). The peptide was suspended in Freund adjuvant (Sigma) supplemented with 3mg/ml of

killed mycobacterium tuberculosis (DIFCO, Detroit, MI). The animals received bilateral intradermal injections of 100 microliters of immunogen in the axillaries and inguinal region. In addition, 3µg/µl of killed *Bordetella pertussis* (Sigma) was administered i.v. on the day of immunization and 48 hours later in order to break down the blood brain barrier and promote the development of the disease. 3,3',-5-triiodothyronine (T3, Sigma), 10mcg/kg, sc, was administered on days 12, 13, 14, 25, 26, 27 post-immunization. Saline was administered to untreated group (vehicle).

Animals were observed daily to record the EAE development and clinical signs using an expanded disabilities scale (23) (see Table II). The clinical signs were characterized by a variety of neurological motility impairments, different sensory parameters and autonomic signals, always associated with weight loss. We applied a score in which 0 meant no symptom and 2 or 3 meant (depending on function) the most severe symptoms. The human end-point was established at value 25 of the neurological disability scale.

Histology, histochemistry and immunohistochemistry

For morphological studies, animals were sacrificed by intracardiac perfusion with saline solution followed by a PBS 0.2 M, pH 6.9 solution containing paraformaldehyde 4% and picric acid 14%. Brains and lumbar spinal cords were dissected out, suitably fixed and sectioned using a cryostat (14µm thickness). Moreover, pieces of spinal cord from animals used for molecular biology experiments were also fixed by immersion in the same fixative for further histological analysis. The extent of inflammation, demyelination and axonal pathology was evaluated on tissue sections stained with hematoxylin and eosin to visualize infiltrate cells and with Sudan Black and FluoroMyelin^{TM} Fluorescence Myelin Staining (Molecular Probes, Eugene, OR) for the myelin sheaths. Indirect immunofluorescence (IF) procedures were used to visualize the anti-tubulin beta III isoform (Chemicon International Inc. Temecula, CA, USA). Sections were first incubated in 0.1 M phosphate buffered saline (PBS) at room temperature for 10-30 min, followed by incubation at 4°C for 24h in a humid atmosphere with the primary antibodies diluted in PBS containing 0.3% Triton X-100, v/v. After rinsing in PBS for 20 min (2x10 min), sections were incubated at 37°C for 30 min in a humid atmosphere with the secondary antisera conjugated with different fluorochromes diluted in PBS/Triton X-100 0.3%. Sections were then rinsed in PBS (as above) and mounted in glycerol containing 1,4-phenylendiamine 0.1 g/l (Sigma). Images were taken by Olympus

AX70-PROVIS microscope equipped with motorized z-stage control and F-VIEW II CCD Camera. Confocal laser scan microscopy (Olympus FV500, Ar/HeNe (G) lasers and appropriate filters for green and red fluorescence) was used to sample beta tubulin III and Fluomyelin staining (Invitrogen, Life Sciences, Milano, Italy). The myelin sheath thickness was measured on confocal images using Image ProPlus software (MediaCybernetics, Bethesda, MD). The G-ratio (ratio of axon diameter to total fibre diameter) was calculated on confocal images by dividing the circumference of an axon without myelin by the circumference of the same axon including myelin. At least 250 fiber/group were included in the analysis. Demyelinated area was measured on Sudan black stained sections and inflammatory infiltrate on hematoxylin and eosin, by delimiting the respective area over the entire white matter using the Analytical Imaging Station software (Imaging Research Inc, St. Catharines, Ont., Canada). Final figures were generated using Adobe Photoshop 6.0 and Adobe Illustrator 9.2 softwares.

Western blotting

Quantitative analysis of myelin basic protein expression was performed by Western blot. The protein concentration in the sample was determined using RC DC protein assay kit (Biorad, Hemel Hempstead, UK). Equal amounts of protein (7μg) from the different samples were separated in 15% SDS-polyacrylamide gels and electroblotted to nitrocellulose membranes (Biorad). In order to block unspecific protein binding sites, filters were incubated with blocking solution (Pierce, Rockford, IL, USA) for 2 hours at room temperature and then with primary antibodies overnight at 4°C. After washing for 1 hour with TTBS (TBS-0.05% Tween-20), blots were incubated with secondary antibodies for 30 min at room temperature and washed again for another hour. Rabbit polyclonal anti-MBP (Dako, Carpenteria, CA, USA) and anti-GAPDH (Chemicon) were used as primary antibody whereas anti-rabbit (1:3000) and anti-mouse (1:1000) immunoglubulins conjugated to horseradish peroxidase (Dako) were used as secondary antibody. Finally, protein bands were detected by exposing ECL (enhanced chemiluminescent) -pre-incubated blots (Pierce) to radiographic films. Molecular weight of proteins was confirmed by comparing sample bands with standard protein marker (Fermentas Life Sciences, Italy). Densitometric analysis was performed using the AIS Imaging System (Ontario, Canada) and the data obtained statistically analyzed and

represented using PrismGraph software (GraphPad Software, San Diego, CA, USA). MBP optical density values were normalized toward GAPDH.

RNA isolation, retrotranscription and real-time semiquantitative PCR

RNA from tissues was prepared following the manufacturer's specifications (mRNA isolation kit for optic nerve and total RNA isolation kit for spinal cord, both from Roche Molecular Biochemical, Mannheim, Germany). RNAs were first subjected to DNase treatment (0.1U/µl, 1xDNase buffer, 4U/µl ribonuclease inhibitor, at 37°C for 30 min) (Fermentas, Life Sciences, Italy) and then reverse transcribed using the M-Moloney murine leukaemia virus (M-MuLV) reverse transcriptase enzyme (10U/µl, 1xfirst strand buffer, 1mM d(NTP)s -Fermentas-, 50µM. $p(dN)_6$ random primers (Roche), 42°C for 60 min). Real-time PCR was performed using the Mx3005P QPCR System (Stratagene, La Jolla, CA, USA) equipped with the FAM™/SYBR® Green I (492nm excitation-516nm emission) filter, among others. The chemistry chosen to perform these real-time PCR experiments was SYBR Green I fluorescent detection and PCRs were performed in a mix reaction consisted of template cDNA, 1xMaster Mix (Stratagene), 16nM ROX reference dye, 0.4µM of both primers, forward and reverse. The primer sequences employed were as follow: D2 forward, 5- ACTTCCTGCTGGTCTACATTG -3, reverse, 5- CCTGGTTCTGGTGCTTCTTC -3; D3 forward, 5- GCGTCTCTATGTCATCCAG -3, reverse, 5- TAGCGTTCCAACCAAGTG -3; TRα1 forward, 5- AGGAGAACAGTGCCAGGTC -3, reverse, 5- ACAAGTGATACAGCGGTAGTG -3; TRα2 forward, 5- TGGACAAAGACGAGCAGTG -3, reverse, 5- GCAGGAATAGGTGGGATGG -3; TRβ1 forward, 5- GCAGGAATAGGTGGGATGG -3, reverse, 5- -3; TRβ2 forward, 5- AGTCCACTGATTATTACGC -3, reverse, 5- AGGTTGGCTGTATTGATTC -3; *Olig-1* forward, 5- AAGTGACCAGAGCGGATG -3, reverse, 5- CCAGGGACAAGGAGAGAG -3; PDGFαR forward, 5- CAGACAGAAGAGAATGAGC -3, reverse, 5- GTGCGACAAGGTATAATGG -3; MBP forward, 5- TGGGAGGAAGAGATAGTC -3, reverse, 5- AGGCAGTTATATTAAGAAGC -3; GAPDH, forward, 5- TCATCCCTGCCTCTACTG -3, reverse, 5- TGCTTCACCACCTTCTTG -3. At the end of the amplification cycles dissociation curves were performed. The thermal profile for the dissociation curve program was the follows: first incubate samples at 95°C for 1 min to denature the PCR amplified products, then ramp temperature down to 55°C and finally

temperature increase from 55°C to 95°C at the rate of 0.2°C/sec, collecting fluorescence data continuously on the 55-95°C temperature ramp. The specificity of amplified products was controlled by both the presence of one peak at the expected melting temperature and the presence of a unique band of the expected size when amplified products were resolved in 2.5% agarose gel and TAE buffer. A 100 bp DNA ladder (Fermentas) was used as DNA marker (Fig. 3 and 6). The relative mRNA level of studied genes was calculated on the basis of threshold cycle (C_T) values obtained from each sample normalized with C_T values of the GAPDH housekeeping gene. Data are expressed as the relative target gene expression in each treated group of animals relative to the control group, obtained by applying the equation: $2^{-\Delta\Delta C_T}$ where $\Delta\Delta C_T = \Delta C_T$ mean value of treated animals - ΔC_T mean value of control animals; ΔC_T treated animals = C_T target gene - C_T GAPDH; ΔC_T control animals = C_T target gene - C_T GAPDH. Samples have been processed in duplicate.

T4, T3, rT3 RIA

Total T3, total T4 and rT3 were measured by radioimmunoassay following the customer protocols (T3 and T4: Immunotech SA, Marseille, France; rT3: Adaltis, Casalecchio di Reno, Italy).

Statistical analysis

All data are expressed as mean ± SEM. The test used in each set of experiments is indicated in each figure legend and in the text, were also the details of the test are reported. Statistics: one-way ANOVA and post-hoc Tukey's multiple comparison test: *$p<0.05$, **$p<0.01$, ***$p<0.0001$; when indicated, two-tailed unpaired Student *t* test was also used: ^{a} $p<0.05$, ^{b} $p<0.01$.

Results

T3 treatment improves EAE clinical course.

Twenty-four marmosets, 13 females and 11 males, were enrolled in the study. All animals were healthy at the beginning of the experiments (clinical status and basic plasma parameters). The mean age of the animals was 59.33+8.90 months (range 11-144) (see Table I). Since marmosets live in stable pairs, both males and females inhabiting the same cage

were immunized. The enrolling strategy allowed experimental groups (control, EAE untreated, EAE treated) to be set up which had comparable sex and mean age composition at the end of the experiment (one way ANOVA, p=0.4020; F = 0.9521) in spite of the wide age-range. The clinical course of EAE was monitored using the neurological disabilities score, including abnormalities of motility (tremor, alert), sensory parameters and autonomic signals (Table II), where 0 means no-symptom and 2/3 means the most severe symptoms for each domain. The ethical end-point was established at value 25 of the marmoset neurological disability scale, which is equivalent to a high disability level in the human MS scale (e.g. EDSS > 7.0). In Table I we reported the details of clinical evolution in each animal, including maximum score and the % body weight loss. The graph in Fig. 1 reports the overall disability score in EAE animals, during the observed time-period and this individual representation was used to calculate the area under the curve for each animal. Symptoms started around 30 days after immunization, showing a peak at day 38, a brief regression and then a chronic progression, which was interrupted by euthanasia at 47 days after immunization in all animals. T3 therapy was started two weeks after disease induction. T3 treatment significantly improved the EAE clinical course, as indicated by the area under the curve (Fig. 2). T3 administration reduced overall disease severity (Fig. 2A) by reducing the percentage of animals developing severe disease (Fig. 2B). We observed that 30% of untreated animals reached score >20, whereas only 10% of T3-treated animals reached this score; conversely, 50% of T3-treated animals reached a score of <10 compared to 30% of untreated animals.

Myelin sheaths are better preserved in EAE marmoset treated with T3 compared to untreated animals.

Post-mortem pathology, as analyzed in the lumbar spinal cord and in the cerebral cortex, confirmed that EAE animals have extensive areas of perivascular and submeningeal inflammation, characterized by abundant cellular infiltrate including mononuclear cells and macrophages, in both the white and grey matter (Fig. 1 A-F, spinal cord; G-N cerebral cortex and corpus callosun). Large areas of demyelination, as identified by histological (Sudan black, Fig. 1 D,F spinal cord; G, cerebral cortex; L, corpus callosum), histochemical (Fluoro-Myelin staining, Fig. 1 N, corpus callosum) and immunohistochemical techniques (immunofluorescence for the myelin basic protein –MBP) were observed in the dorsal and ventral funiculi and in the peripheral part of the white matter. Both clinical course and

pathology of EAE marmoset corresponded to the standard course of the disease (23), and most of the observed lesions can be classified as active (hypercellular).

Due to ethical reasons, this is a single time-point study. Since spontaneous remyelination occurs in EAE, it is hard to distinguish if the effect of the TH treatment is related to the myelin sheath preservation or to an improved repair. We then used the term demyelination/remyelination balance throughout the paper. We analyzed demyelination/remyelination balance in EAE marmosets treated with T3 or saline by means of molecular, immunohistochemical and morphological techniques. We first focused on the study of expression changes of three genes reflecting OPCs at different maturation stages, in the spinal cord, the optic nerve (Fig. 3) and cerebral cortex (Fig. 4). Platelet-derived growth factor α receptor (PDGFαR) is a marker for OPCs, and its mRNA expression slightly increases in the spinal cord, but not in the optic nerve, of EAE animals. Conversely, MBP expression (mRNA and protein), which reflects a mature stage of the oligodendrocyte, is down-regulated during EAE. T3 administration increases PDGFα mRNA expression in both spinal cord and optic nerve, and restores the capability to produce MBP in the spinal cord. Moreover, it up-regulates mRNA expression of Olig-1 in the optic nerve, which is one of the early genes expressed by neural stem cells during oligodendroglial lineage.

We also analyzed these markers in the cerebral cortex, profiting of the fact that the marmoset model has cortical lesions similar to humans (24). Demyelination plaques were observed in the white matter of the corpus callosum, and these white matter lesions extend into the cortex together with an inflammatory infiltrate (Fig. 1 G, L-N). These lesions can be classified as leukocortical lesions (25). Also in the cerebral cortex as sampled in fronto-medial areas, there is a decline in MBP synthesis during EAE, which is completely restored by T3 treatment (Fig. 4).

In order to establish if molecular regulations observed in animals suffering EAE correspond to a structural protection or repair, we analyzed the white tracts in 1 cm of the lumbar spinal cord in control, EAE-untreated and T3-EAE-treated animals by quantitative morphometric analysis. Representative sections from control, EAE and EAE-T3 treated animals histochemically stained with fluomyelin are reported in Fig. 5, A-C. Sudan black stained coronal sections were used for serial analysis, whereas fluomyelin histochemistry and MBP-immunohistochemistry were performed at established intervals (every 200 microns). The demyelinated area over the entire section (dorsal, ventral and lateral funiculi) was measured in

60 sections/animal. Quantitative analysis indicates higher myelinated area in T3-treated animals with respect to the untreated animals (Fig. 5D). We also performed the analysis of myelin sheath thickness in the fascilus gracilis (white square in A) on the fluomyelin stained section sampled by confocal microscopy, also calculating the G-ratio. We included in the analysis fibres with an external diameter ranging from 5 to 11 microns, which correspond to the diameter of touch fibres. The mean thickness of the sampled sheaths, which is decreased in EAE, is preserved in T3 treated animals (Fig. 5G-I). The G-ratio was higher in vehicle-treated EAE than in T3-treated EAE (Fig. 5E), even if the T3-treatment does not restore control values.

In order to investigate the possible effect of T3 treatment on overall tissue inflammation, we analyzed tissue inflammation by measuring the percentage area infiltrated by cells over the entire white matter, finding that T3-treatment reduces this score (Fig. 5F).

Finally, in order to explore axon pathology, we also analysed the density of beta-tubulin-IR axons in the same area, observing that beta-tubulin immunoreactivity is almost destroyed in EAE, while is preserved in animal treated with T3 (Fig. 5L-N).

Thyroid function and tissue metabolism of TH are altered in EAE and normalized by T3 treatment.

Plasma levels of thyroid hormones at the time of sacrifice are reported in Table III. There was a severe reduction in both T3 and T4 plasma levels in EAE compared to control animals, and an increase in rT3. T3 treatment restored T3, T4, rT3 plasma levels without inducing hyperthyroidism.

In order to explore the hypothesis that an alteration in cellular effectors for TH action is present in the CNS in EAE, we investigated the mRNA expression level of type 2 (D2) and type 3 (D3) deiodinase, and of of nuclear TH receptor isoforms, i.e. alfa1 (TRα1), alpha2 (TRα2), beta1 (TRβ1), beta2 (TRβ2) by means of real time PCR in the spinal cord. Results are reported in Fig. 6 and expressed as relative expression in folds of increase or decrease of EAE and EAE-T3 *vs* control animals. In EAE animals, we found an increase in D2 mRNA and a reduction in TRβ1 and TRβ2 mRNA levels. T3 treatment induced a strong increase in D3 mRNA expression, thus confirming the long-lasting impact of T3 treatment on pathological tissue, reduced D2 mRNA expression and restored TRβ1 and TRβ2 mRNAs to control expression levels. Results from statistical analysis are reported in the figure legend.

Discussion

Thyroid hormone administration protects myelin sheath integrity and ameliorates clinical course in EAE marmoset

Previous results from our and other laboratories have indicated that thyroid hormone administration has a positive effect on clinical outcome and demyelination/remyelination balance in rodent models of inflammatory-demyelinating diseases, i.e. EAE in rat and cuprizone demyelination in mouse and rat. Here we extended these findings to the MS model in the non-human primate *C. jacchus* (marmoset), showing that pulsed T3 administration improves clinical outcome, protects myelin sheath integrity, and restores molecular indices of myelin basic protein production. The common marmoset is a small monkey sharing neuroanatomical and molecular similarity with the human brain (ratio of white matter to grey matter, expression of growth factors, etc.). Marmoset EAE shares key neuropathological features with MS, such as the sequence of immune and inflammatory events and white matter lesions. Furthermore, the EAE induced in the marmoset, but not in the mouse and rat, display human-like MS grey matter pathology, including cortical lesions, cortical atrophy (24), and early axonal damage (26). These general features, in addition to its outbred nature and its well-established genetic and immunological similarity to humans, make the marmoset an attractive animal model in neurological diseases and MS.

The effect of exogenous T3 administration on EAE might involve different cell types and pathogenic processes, starting from inflammatory and immune cells. In fact, we observed a reduction of the inflammatory cellular infiltrate in the spinal cord of T3-treated EAE animals. The immune cells contain T3 (27), supporting the view of a complex and still poorly understood interaction between TH and immune function (28). It has been recently showed that thyroxine inhibits macrophage migration in a model of sepsis by targeting a specific protein (29). TH also regulates the expression of cytoskeleton protein during axon growth and regeneration (30), thus indirectly modulating the axon-oligodendrocyte interplay that provides for proper white matter development, organization and repair. Finally, TH regulates several aspects of astrocyte differentiation and maturation, including the production of extracellular matrix proteins and growth factors, and thus controls neuronal growth and neuritogenesis (31).

The reduction of inflammation could explain the improvement in clinical status, but in our opinion is much more difficult to explain the regulation of OPCs genes and proteins as a consequence of inflammation. Moreover, while knowledge on the possible role of TH in regulating inflammation and immune function is still poor, extensive evidences have been accumulated over the past decades on the role of TH on OPC maturation and myelination. Thus, we focused our attention on OPCs, the remyelinating cell in mature CNS (2). Existing OPCs actively proliferate under proinflammatory cytokine drive (2,32) and new remyelinating cells are also generated from neural stem cells (33,34) in different CNS injury models. We observed that the expression of the OPC marker PDGFα□ mRNA slightly increases in the spinal cord in EAE marmoset, thus suggesting that OPC proliferation occurs in the marmoset. T3 administration also induces a slight increase in the expression of the transcription factor Olig1 in the optic nerve, which could suggest that new OPCs are generated (35,36). Olig1 up-regulation is required to repair demyelinated lesions (37). We also observed a further increased in PDGFα□ (OPC) mRNA expression after T3 treatment, thus supporting the hypothesis that in the presence of a proliferation drive (i.e. pro-inflammatory cytokines), exogenous T3 is able to trigger the generation of new OPCs from NSCs, as also shown by in vitro studies (15).

The subsequent step in remyelination requires that OPCs differentiate into myelinating oligodendrocytes. This process is regulated by two functional components: the so-called timing component, which depends on platelet-derived growth factor (PDGF) and other mitogens, which induce cells to divide, and the effector component, which is regulated by T3 (38). T3 causes the cell to withdraw from the cell cycle and to undergo terminal differentiation by acting through the nuclear receptors. In the presence of PDGF, but without T3, OPCs proliferate with no chance of evolving into mature oligodendrocytes (39). Notably, also in vivo studies in mice lacking TRs indicates that TR gene products are necessary to ensure terminal differentiation of OPC into myelinating oligodendrocytes (40). A differentiation block of OPCs seems to be the major determinant of remyelination failure in chronic MS lesions (5). This step seems to be altered also in the EAE marmoset, as suggested by increased expression of PDGFα□ mRNA, but impaired expression of MBP, which is the most abundant protein in the myelin sheaths synthesized by mature oligodendrocytes. As in the rat, T3 administration seems to restore the capability to produce MBP in both the white and the grey matter in EAE marmoset. However, since the expression of gene encoding for

the three major myelin proteins by mature oligodendrocytes is TH-dependent as well, and TRs binding sites have been identified on myelin protein encoding genes using ChIP-on-Chip (41), the observed up-regulation of MBP mRNA and protein level after T3 could also derive from resident oligodendrocytes. The morphological and morphometric analysis of the confocal images of flyomyelin-stained fibres points to a substantial preservation of myelin sheath morphology and a normal thickness, thus suggesting that the whole remyelination process and/or myelin sheath protection from inflammatory attack benefit from T3 administration. Finally, preliminary data from the morphological analysis of the axons indicates that T3 administration also limits axonal damage in marmoset as well as in rat EAE (17).

Inflammation alters thyroid function and tissue expression of cellular effectors of thyroid hormone action: a case of non-thyroidal illness syndrome?

To explore possible mechanisms underlying the positive effect of T3, we investigated the thyroid hormone function at systemic and cellular level during EAE.

While T4 is the principal product of the thyroid gland and the most abundant circulating TH, T3 is the active form and rT3 the inactive one. Plasma T3 is 80 % derived from extrathyroidal conversion of T4 into T3 by tissue-specific selenoprotein iodothyronine deiodinases (Ds), and the rT3 is produced outside the thyroid gland. D2 is the active deiodinase isoform in the brain, which is responsible for the production of 75% of brain T3 (42), whereas D3 converts T4 and T3 into the inactive rT3 and 3,3'T2, thus locally protecting against hyperthyroidism. Most classic TH actions are actually genomically mediated by T3 binding to four different nuclear receptors (TRs) belonging to to the nuclear receptor superfamily and act as transcription factors for target genes (43). Thus, the biological activity of TH on target cells including OPCs, is determined by intracellular T3 concentration, which is dependent on plasma levels, on the expression of transporters on the plasma membrane, on the expression and activity of deiodinases, and, on the expression of nuclear receptors.

In marmosets affected by the inflammatory-demyelinating disease EAE, there is a drastic decrease in plasma T3 and T4, and a rise in plasma rT3. This is not surprising, since for more than 3 decades it has been a known fact that serum TH decreases during severe illness, and inflammatory responses are associated with profound changes in thyroid hormone metabolism, a condition collectively known in humans as "non thyroidal illness syndrome"

(NTIS) (44,45). In mild illness this involves only a decrease in serum T3 level. However, as the severity of the illness increases, there is a drop in both serum T3 and T4, and rT3 rises, whereas TSH is abnormal in only 10% of cases.

Mechanisms underlying altered thyroid function during severe diseases including inflammation are still disputed. In EAE, this could be due to direct hypothalamic inflammation involving thyreotropic releasing hormone-containing neurons in the paraventricular nucleus of the hypothalamus. Deep grey matter inflammation affecting also the hypothalamus has actually been described in experimental central inflammation (46) and MS (47). Moreover, in spite of the fact that care was taken to ensure marmosets had a proper food intake, a 20% body weight decrease was observed in most of the animals. Malnutrition is thus a possible component of chronic disease, capable of inducing a different functional set-up of the hypothalamus-pituitary-thyroid axis (45).

Alternatively or complementary to this, systemic hypothyroid state could be related to complex feedback regulation associated with the cellular utilization of THs involving deiodinases and nuclear receptors. Otherwise, the tissue hypothyroidism could be un-related to hypothalamic regulation. Much of current research suggests in fact that proinflammatory cytokines, including interleukin 1β and TNFα, which are key mediators of tissue inflammation also in EAE, may reduce T3 signaling due to D2 inhibition, to increased D3 activity or to a dysregulation of TRs expression (44,48). Tissue expression of Ds and TRs is severely altered in EAE marmoset. For example, expression of D2 mRNA increases in the spinal cord. This could be the reflection of a tissue reaction to hypothyroidism, since in many tissues, including the CNS, D2 mRNA expression is regulated in such a way as to maintain constant local T3 levels in the presence of decreased D2 activity (49). However, brain injury itself and immune activation increase D2 mRNA expression and decrease its activity (50,51). A marked expression of D3 by granulocytes and macrophages in spinal cord inflammatory lesions has been described during EAE (52). Increased D3 expression could theoretically result in decreased T3 availability, and thus local tissue hypothyroidism.

A dysregulation of TR expression has been described in several cell types during inflammation (53,54). We have observed that the expression of TRβ isoforms declines in EAE and is restored (TRβ1) or even upregulated (TRβ2) in EAE marmosets treated with T3. Indeed, the expression of TRβ1 and TRβ2 decreases, as has also been described in the skeletal muscle of patients with NTIS (55), whereas D2 expression increases, as described in

a rabbit model of prolonged critical illness (56). Thus, the lower TR expression found in EAE might also be involved in impaired T3 action in tissue.

In conclusion, we suggest that these alterations in CNS conversion and nuclear action of TH, such as systemic hypothyroidism, might negatively affect cellular and molecular events strictly regulated by TH, such as OPCs conversion into myelinationg oligos and myelin protein gene expression. T3 replacement therapy could reverse these defects, but also affect inflammation. Although there are few indications regarding possible systemic thyroid hormone dysfunction in MS also due to thyroid dysfunctions frequently induced by MS therapies (e.g. interferon beta1), in a small-scale study on MS low serum T3 concentrations coexisting with normal T4 levels have been described (57). Moreover, a higher rT3 and TT4/rT3 ratio has been described in the cerebrospinal fluid of 38 MS patients, thus supporting an abnormal thyroid hormone metabolism in the CNS of these patients (58). Notably, the proteomic analysis of chronic active plaques revealed that TRs expression is severely altered in MS patients (59).

Acknowledgements

This work was supported by Regione Emilia Romagna, PRRIITT projects (LC) and by Italian Multiple Sclerosis Foundation (LG); Centro di Fisiopatologia del Sistema Nervoso, Modena (LC); IRET-ONLUS Foundation (LG), Bologna. Authors extend special thanks to Dr. Luigi Aloe, Institute for Neurobiology and Molecular Medicine, CNR, Roma, for helping in obtaining the marmoset experiment approval; Mrs. Nadia De Sordi, DIMORFIPA, University of Bologna for technical support in histology and histochemistry.

References

1. Stadelmann C, Wegner C, Bruck W. Inflammation, demyelination, and degeneration – Recent insights from MS pathology. *Biochimica et Biophysica Acta* 2011; **1812**: 275-282.
2. McTigue DM, Tripathi RB. The life, death, and replacement of oligodendrocytes in the adult CNS. *J Neurochem* 2008; **107**: 1-19.
3. Nait-Oumesmar B, Picard-Riera N, Kerninon C, Decker L, Seilhean D, Höglinger GU, Hirsch EC, Reynolds R, Baron-Van Evercooren A. Activation of the subventricular zone in multiple sclerosis: evidence for early glial progenitors. *Proc Natl Acad Sci USA* 2007; **104**: 4694-4699.
4. Wilson HC, Scolding NJ, Raine CS. Co-expression of PDGF alpha receptor and NG2 by oligodendrocyte precursors in human CNS and multiple sclerosis lesions. *J Neuroimmunol* 2006; **176**: 162-173.
5. Kuhlmann T, Miron V, Cui Q, Wegner C, Antel J, Bruck W. Differentiation block of oligodendroglial progenitor cells as a cause for remyelination failure in chronic multiple sclerosis. *Brain* 2008; **131**: 1749-1758.
6. Lubetzki C, Williams A, Stankoff B. Promoting repair in multiple sclerosis: problems and prospects. *Curr Opinion Neurol* 2005; **18**: 237-2344.
7. Miller RH, Mi S. Dissecting demyelination. *Nature Neurosci* 2007; **10**: 1351-1354.
8. Bernal J. Action of thyroid hormone in brain. *J Endocrinol Invest* 2002; **25**: 268-288.
9. Zoeller RT, Rovet J. Timing of thyroid hormone action in the developing brain: clinical observations and experimental findings. *J Neuroendocrinol* 2004; **16**: 809-818.
10. Horn S, Heuer H. Thyroid hormone action during development: More questions than answer. *Molecular Cell Endocrinol* 2010; **315**: 19-26.
11. O'Shea PJ, Williams GR. Insight into the physiological actions of thyroid hormone receptors from genetically modified mice. *J Endocrinol* 2002; **175**: 553-570.
12. Babu S, Sinha RA, Mohan V, Rao G, Pal A, Pathak A, Singh M, Godbole MM. Effect of hypothyroxinemia on thyroid hormone responsiveness and action during rat postnatal neocortical development. *Exp Neurol* 2011; **228**: 91-98.
13. Baas D, Bourbeau D, Sarlième LL, Ittel ME, Dussault JH, Puymirat J. Oligodendrocyte maturation and progenitor cell proliferation are independently regulated by thyroid hormone. *Glia* 1997; **19** :324-332.

14. Fernández M, Pirondi S, Manservigi M, Giardino L, Calzà L. Thyroid Hormone participates in the regulation of neural stem cells and oligodendrocyte precursor cells in the central nervous system of adult rat. *Eur J Neurosci* 2004; **20**: 2059-2070.
15. Fernández M, Paradisi M, Del Vecchio G, Giardino L, Calzà L. Thyroid hormone induces glial lineage of primary neurospheres derived from non-pathological and pathological rat brain: implications for remyelination-enhancing therapies. *Int J Dev Neurosci* 2009; **27**: 769-778.
16. Calzà L, Fernandez M, Giuliani A, Aloe L, Giardino L. Thyroid hormone activates oligodendrocyte precursors and increases a myelin-forming protein and NGF content in the spinal cord during experimental allergic encephalomyelitis. *Proc Natl Acad Sci USA* 2002; **99**: 3258-3263.
17. Fernandez M, Giuliani A, Pirondi S, D'Intino G, Giardino L, Aloe L, Levi-Montalcini R, Calzà L. Thyroid hormone administration enhances remyelination in chronic demyelinating inflammatory disease. *Proc Natl Acad Sci USA* 2004b; **101**: 16363-16368.
18. Giardino L, Giuliani A, Fernandez M, Calzà L. Spinal motoneuron distress during experimental allergic encephalomyelitis. *Neuropathol Appl Neurobiol* 2004; **30**: 522-531.
19. Calzà L, Fernandez M, Giardino L. Cellular approaches to central nervous system remyelination stimulation: thyroid hormone to promote myelin repair via endogenous stem and precursor cells. *J Mol Endocrinol* 2010; **44**: 13-23.
20. Pluchino S, Muzio L, Imitola J, Deleidi M, Alfaro-Cervello C, Salani G, Porcheri C, Brambilla E, Cavasinni F, Bergamaschi A, Garcia-Verdugo JM, Comi G, Khoury SJ, Martino G. Persistent inflammation alters the function of the endogenous brain stem cell compartment. *Brain* 2008; **131**: 2564-2578.
21. Franco PG, Silvestroff L, Soto EF, Pasquini JM. Thyroid hormones promote differentiation of remyelination after cuprizone-induced demyelination. *Exp Neurol* 2008; **212**: 458-467.
22. Harsan LA, Steibel J, Zaremba A, Agin A, Sapin R, Poulet P, Guignard B, Parizel N, Grucker D, Boehm N, Miller RH, Ghandour MS. Recovery from chronic demyelination by thyroid hormone therapy: myelinogenesis induction and assessment by diffusion tensor magnetic resonance imaging. *J Neurosci* 2008; **28**: 14189-14201.
23. Villoslada P, Hauser SL, Bartke I, Unger J, Heald N, Rosenberg D, Cheung SW, Mobley WC, Fisher S, Genain CP. Human nerve growth factor protects common marmosets

against autoimmune encephalomyelitis by switching the balance of T helper cell type 1 and 2 cytokines within the central nervous system. *J Exp Med* 2000; **191**: 1799-1806.

24. Pomeroy IM, Matthews PM, Frank JA, Jordan EK, Esiri MM. Demyelinated neocortical lesions in marmoset autoimmune encephalomyelitis mimic those in multiple sclerosis. *Brain* 2005; **128**: 2713-2721.
25. Kap YS, Laman JD, 't Hart BA. Experimental autoimmune encephalomyelitis in common marmoset, a bridge between rodent EAE and multiple sclerosis for immunotherapy development. *J Neuroimmune Pharmacol* 2010; **5**: 220-230.
26. Mancardi G, Hart B, Roccatagliata L, Brok H, Giunti D, Bontrop R, Massacesi L, Capello E, Uccelli A. Demyelination and axonal damage in a non-human primate model of multiple sclerosis. *J Neurol Sci* 2001; **184**: 41-49.
27. Pallinger E, Csaba G. A hormone map of human immune cells showing the presence of adrenocorticotropic hormone, triiodothyronine and endorphin in immunophenotyped white blood cells. *Immunology* 2008; 123:584-589.
28. Klecha AJ, Klecha AJ, Genaro AM, Gorelik G, Barreiro Arcos ML, Silberman DM, Schuman M, Garcia SI, Pirola C, Cremaschi GA. Integrative study of hypothalamus-pituitary-thyroid-immune system interaction: thyroid hormone-mediated modulation of lymphocyte activity through the protein kinase C signaling pathway. *J Endocrinol* 2006; **189**: 45-55.
29. Al-Abed Y, Metz CN, Cheng KF, Aljabari B, Vanpatten S, Blau S, Lee H, Ochani M, Pavlov VA, Coleman T, Meurice N, Tracey KJ, Miller EJ. Thyroxine is a potential endogenous antagonist of macrophage migration inhibitory factor (MIF) activity. *Proc Natl Acad Sci USA* 2011; **108**:224-8227.
30. Shenker M, Riederer BM, Kuntzer T, Barakat-Walter I. Thyroid hormones stimulate expression and modification of cytoskeletal protein during rat sciatic nerve regeneration. *Brain Res* 2002; **957**: 259-270.
31. Trentin AG. Thyroid hormone and astrocyte morphogenesis. *J Endocrinol* 2006; **189**: 189-197.
32. Reynolds R, Dawson M, Papadopulos D, Polito A, Di Bello IC, Pham-Dinh D, Levine J. The response of NG2-expressing oligodendrocyte progenitors to demyelination in MOG-EAE and MS. *J Neurocytol* 2002; **31**: 523-536.

33. Calzà L, Giardino L, Pozza M, Bettelli C, Micera A, Aloe L. Proliferation and phenotype regulation in the subventricular zone during experimental encephalomyelitis in vivo evidence of a role for nerve growth factor. *Proc Natl Acad Sci USA* 1998; **95**: 3209-3214.
34. Picard-Riera N, Decker L, Delrasse C, Goude K, Nait-Oumesmar B, Liblau R, Pham-Dinh D, Evercooren AB: Experimental autoimmune encephalomyelitis mobilizes neural progenitors from the subventricular zone to undergo oligodendrogenesis in adult mice. *Proc Natl Acad Sci USA* 2002; **99**: 13211-13216.
35. Jakovcevski I, Zecevic N. Olig transcription factors are expressed in oligodendrocyte and neuronal cells in human fetal CNS. *J Neurosci* 2005; **25**: 10064-10073.
36. Emery B. Regulation of oligodendrocyte differentiation and myelination. *Science* 2010; **330**: 779-782.
37. Arnett HA, Fancy SP, Alberta JA, Zhao C, Plant SR, Kaing S, Raine CS, Rowitch DH, Franklin RJ, Stiles CD. bHLH transcription factor Olig1 is required to repair demyelinated lesions in the CNS. *Sicence* 2004; **306**: 2111-2115.
38. Tang DG, Tokumoto YM, Raff MC. Long-term culture of purified postnatal oligodendrocyte precursor cells. Evidence for an intrinsic maturation program that plays out over months. *J Cell Biol* 2000; **148**: 971-984.
39. Durand B, Raff M. A cell-intrinsic timer that operates during oligodendrocyte development. *BioAssays* 2000, 22:64-71.
40. Baas D, Legrand C, Samarut J, Flamant F: Persistence of oligodendrocyte precursor cells and altered myelination in optic nerve associated to retina degeneration in mice devoid of all thyroid hormone receptors. *Proc Natl Acad Sci USA* 2002; **99**: 2907-2911.
41. Dong H, Yauk CL, Rowan-Carroll A, You S-E, Zoeller T, Lambert I, Wade MG. Identification of thyroid hormone receptor binding sites and target genes using ChIP-on-Chip in developing mouse cerebellum. *PLoS ONE* 2009; **4**: e4610.
42. Bianco AC, Salvatore D, Gereben B, Berry MJ, Larsen PR. Biochemistry, cellular and molecular biology, and physiological roles of the iodothyronine selenodeiodinases. *Endocrinol Rev* 2002; **23**: 38-89.
43. Cheng S-Y, Leonard JL, Davis PJ. Molecular aspects of thyroid hormone actions. *Endocrine Rev* 2010; **31**: 139-170.
44. Koenig RJ. Modeling the nonthyroidal illness syndrome. *Curr Opin Endocrinol Diabetes Obes* 2008; **15**: 466-469.

45. Warner MH, Beckett GJ. Mechanisms behind the non-thyroidal illness syndrome: an update. *J Endocrinol* 2010; **205** :1-13.
46. Boelen A, Kwakkel J, Wiersinga WM, Fliers E. Chronic local inflammation in mice results in decreased TRH and type 3 deiodinase mRNA expression in the hypothalamic paraventricular nucleus independently of diminished food intake. *J Endocrinol* 2006; **191**: 707-714.
47. Vercellino M, Masera S, Lorenzatti M, Condello C, Merola A, Mattioda A, Tribolo A, Capello E, Mancardi GL, Mutani R, Giordana MT, Cavalla P. Demyelination, inflammation, and neurodegeneration in multiple sclerosis deep gray matter. *J Neuropathol Exp Neurol* 2009; **68**: 489-502.
48. Baur A, Bauer K, Jarry H, Köhrle J. Effects of proinflammatory cytokines on anterior pituitary 5'-deiodinase type I and type II. *J Endocrinol* 2000; **167**: 505-515.
49. Kwakkel J, Wiersinga WM, Boelen A. Differential involvement of nuclear factor-kappaB and activator protein-1 pathways in the interleukin-1beta-mediated decrease of deiodinase type 1 and thyroid hormone receptor beta1 mRNA. *J Endocrinol* 2006; **189**: 37-44.
50. Fekete C, Gereben B, Doleschall M, Harney JW, Dora JM, Bianco AC, Sarkar S, Liposits Z, Rand W, Emerson C, Kacskovics I, Larsen PR. Lipopolysaccharide induces type 2 iodothyronine deiodinase in the mediobasal hypothalamus: implications for the nonthyroidal illness syndrome. *Endocrinology* 2004; **145**: 1649-1655.
51. Margaill I, Royer J, Lerouet D, Raumagé M, Le Goascogne C, Li WW, Plotkine M, Pierre M, Courtin F. Induction of type 2 iodothyronine deiodinase in astrocytes after transient focal cerebral ischemia in the rat. *J Cereb Blood Flow Metab* 2005; **25**: 468-476.
52. Boelen A, Mikita J, Boiziau C, Chassande O, Fliers E, Petry KG. Type 3 deiodinase expression in inflammatory spinal cord lesions in rat experimental autoimmune encephalomyelitis. *Thyroid* 2009; **19**: 1401-1406.
53. Boelen A, Kwakkel J, Platvoet-ter Schphorst M, Boelen A. Interleukin-18, a proinflammatory cytokine, contributes to the pathogenesis of non-thyroidal illness mainly via the central part of the hypothalamus-pituitary-thyroid axis. *Eur J Endocrinol* 2004; **151**: 497-502.
54. Kwakkel J, Wiersinga WM, Boelen A. Interleukin-1beta modulates endogenous thyroid hormone receptor alpha gene transcription in liver cells. *J Endocrinol* 2007; **194**: 257-265.

55. Lado-Abeal J, Romero A, Castro-Piedras I, Rodriguez-Perez A, Alvarez-Escudero J. Thyroid hormone receptors are down-regulated in skeletal muscle of patients with non-thyroidal illness syndrome secondary to non-septic shock. *Eur J Endocrinol* 2010; **163**: 765-773.
56. Mebis L, Debaveye Y, Ellger B, Derde S, Ververs EJ, Langouche L, Darras VM, Fliers E, Visser TJ, Van den Berghe G. Changes in the central component of the hypothalamus-pituitary-thyroid axis in a rabbit model of prolonged critical illness. *Crit Care* 2009; **13**: R147.
57. Zych-Twardowska E, Wajgt A. Blood levels of selected hormones in patients with multiple sclerosis. *Med Sci Monit* 2001; **7**: 1005-1012.
58. Jiang Y, Yang Y, Zhang B, Peng F, Bao J, Hu X. Cerebrospinal fluid levels of iodothyronines and nerve growth factor in patients with multiple sclerosis and neuromyelitis optica. *Neuoendocrinol Lett* 2009; **30**: 85-90.
59. Han MH, Hwang S-II, Roy DB, Lundgren DH, Price JV, Ousman SS, Fernald GH, Gerlitz B, Robinson WH, Baranzini SE, Grinnell BW, Raine CS, Sobel RA, Han DK, Steinman L. Proteomic analysis of active multiple sclerosis lesions reveals therapeutic targets. *Nature* 2008; **451**: 1076-1081.

Figure Legends

Fig 1.

Clinical evolution and histopathology landmarks of EAE. The graph reports the clinical score of the disease in vehicle-treated marmoset, as evaluated by the expanded disability neurological scale presented in Table II. The arrows indicate the days on which T3 was administered. Micrographs illustrate inflammation and demyelination in the spinal cord and cortex of EAE animals. In particular: A, transverse section of lumbar spinal cord of EAE marmoset stained by hematoxylin eosin; B, C, E, high-power micrographs from the same staining illustrating perivascular and parenchymal infiltration by mononuclear cells and macrophages of inflammatory cells. The asterisk indicates a vessel. D: transverse section of lumbar spinal cord of EAE marmoset stained by Sudan black to show demyelination. The dark areas in the white matter indicate intact myelin, whereas the weaker stained, peripheral areas indicate demyelination (see black arrow); high-power micrographs in E and F illustrate the overlap of inflammation (E) and demyelination (F). (G) coronal section of the cerebral cortex (cingulated region) showing large perivascular demyelination plaques in the corpus callosum (cc, Sudan black weakly stained area, delimitated by the black line), corresponding to inflammatory infiltrates (H, hematoxylin and eosin staining) also containing mononuclear cells (I). (L-N) Micrographs show a typical plaque in the cerebral cortex, showing demyelination (L: the Sudan black staining is lacking; N: the fluorescence fluomyelin staining is lacking, as indicated by the black area) and inflammation (M: hematoxylin and eosin staining). Bar: 100μm

Fig 2.

(A) The graph reports the overall clinical score in EAE and EAE-T3 marmoset, as calculated by the area under the curve describing the time-course evolution of the disease, showing that T3-treatment reduces the severity of the disease. Statistical analysis: Student's t test, $p=0.0433$. (B) The graph reports the percentage of animals in different classes of severity, e.g. <10, 10-20, >20, showing that disease severity in EAE animals treated with T3 is shifted toward a less severe disease compared to untreated animals.

Fig 3.

Expression level of oligodendrocyte markers in the lumbar spinal cord and the optic nerve. *Olig-1,* PDGFαR and MBP mRNA levels were studied in both areas by real-time PCR. Results are expressed as relative gene expression referred to control group of animals (lumbar spinal cord) and/or EAE group (optic nerve), from data obtained by using the equation $2^{-\Delta\Delta C}{}_{T}$. Results are presented as mean ± SEM. Statistical analyses performed: one-way ANOVA with post-hoc Tukey's comparison test (indicated by asterisk *) and two-tailed unpaired Student's *t* test (indicated by letters [a]). Spinal cord: (A) no difference were observed in *Olig-1* mRNA between control and EAE, while T3-treatment significantly increased *Olig-1* mRNA level (*p=0.0381), also in the case of PDGFα□ mRNA (B) (**p=0.0095). (C) The level of MBP mRNA was decreased in EAE and restored to control level after T3-treatment (*p=0.0443). (E) The MBP protein expression decreased in EAE group was restored to control value by T3-treatment (*p=0.0014). (D) Target genes PCR product resolved in agarose gel are included in the figure: line 1, 100 bp ladder DNA marker; line 2, MBP; line 3, PDGFα□; line 4, *Olig-1*. (F) A representative Western blot showing bands corresponding to 18.5 kDa isoform MBP protein in control, EAE and EAE+T3 groups of animals has been included in the figure. Optic nerve: *Olig-1 (G)*, PDGFα□ (H) and MBP (I) mRNA expression level, respectively, in control, vehicle-treated and T3-treated EAE animals. Results are normalized vs control group in graphs G-I. The results obtained when comparing EAE+T3 with EAE group are included in graphs J-L. Statistical analysis: one-way ANOVA with post-hoc Dunnett's comparison test, *p>0.05, **p>0.01, ***p>0.001. Statistical analysis: two-tailed unpaired Student's *t* test: J, *Olig-1* mRNA, [a] p=0.0385); K, PDGFα□ mRNA , [a] p=0.0130 and L, MBP mRNA , [a] p=0.0353.

Fig. 4.

Oligodendrocyte marker expression in the cerebral cortex. The levels of PDGFαR (A) and MBP mRNA (B) were studied by real-time PCR. No differences were observed for PDGFαR mRNA whereas MBP mRNA level significantly decreased in EAE group and T3 treatment restored it to control level. (C) Changes observed in the MBP protein expression (18.5 KDa isoform) studied by Western blot were in the same direction as the MBP mRNA. Data expressed as mean+SEM. Statistical analyses performed: A-B, one-way ANOVA with post-hoc Tukey's comparison test, *p<0.05; **p<0.01; ***p<0.001

Fig 5.

Morphometric analysis of demyelination/remyelination (A-H) and axonal pathology (I-M) in EAE and EAE+T3-treated animals. The low power micrographs illustrate sample sections of the lumbar spinal cord stained for myelin visualization (fluomyelin histochemistry) in control (A), EAE (B) and EAE+T3 animals. The oval in C indicates a residual demyelinated area. Intact myelin is visualized as white signal, whereas the dark areas in B indicate extensive demyelination in dorsal funiculus and peripheral areas of the white matter (see asterisk). (D); overall morphometric evaluation of demyelination in the lumbar spinal cord of EAE and EAE-T3-treated animals, showing the positive effects of T3 treatment (mean+SEM). Statistical analysis: two-tailed unpaired Student's *t* test *$p<0.05$. (H): axon diameter/fiber diameter (g ratio) showed a significant increase in vehicle-EAE animals and a significant decrease in T3-EAE animals, although the mean value in these animals is still higher than in controls. Statistical analysis: one-way ANOVA with post-hoc Dunnett's comparison test, *$p<0.05$; $p<0.001$; (F) evaluation of cellular infiltrate: T3 treatment lowers the extension of cellular infiltrate. Statistical analysis: two-tailed unpaired Student's *t* test *$p<0.05$; (G-I): confocal images of the myelin sheaths in the dorsal funiculus of control and experimental animals, showing the severe disaggregation of the white matter in EAE animals. The numbers inserted indicate myelin sheath thickness as evaluated in a 41753μm2 square area (6 areas/animal), showing a positive effect of T3 treatment. Statistical analyses: one-way ANOVA with post-hoc Dunnett's comparison test, *$p<0.05$; (L-N): micrographs of the axons in the dorsal funiculus, showing the disaggregation of beta-tubulin during EAE, and the restitution by T3. The numbers inserted indicate the number of detectable axons in a 36475μm2 square area (6 areas/animal), proving the positive effect of T3 treatment. Statistical analyses: one-way ANOVA with post-hoc Dunnett's comparison test, *$p<0.05$.

Fig. 6.

(A-G). Deiodinases (A,B) and thyroid hormone receptor (D-G) mRNA expression in the lumbar spinal cord in EAE and EAE-T3 treated animals. Results are expressed as relative gene expression referred to control group (x-fold of control). (A) EAE induced a significant increase in D2 mRNA (*p=0.0165); (B) D3 mRNA level was increased in EAE+T3 (***p<0.001). (D-G) Thyroid hormone receptor subtypes α-1, α-2, β-1 and β-2 mRNA levels were not significantly different when comparing control with EAE and EAE+T3 groups. (F) A significant difference was found in TRβ-1 mRNA expression between EAE and EAE+T3 group (*p=0.042). (G) TRβ-2 mRNA level was also increased in EAE+T3 comparing with EAE group of animals (**p=0.0029). (C) Agarose gel with PCR products of studied target genes: line 1, D3; line 2, D2; line 3, 100 bp ladder DNA marker, used to estimate the size of PCR products obtained; line 4, TRα-1; line 5, TRα-2; line 6, TRβ-1; line 7, TRβ-2. Results are presented as mean ± SEM, samples have been processed in duplicate. Statistical analyses were performed by using one-way ANOVA with post-hoc Tukey's comparison test (*p<0.05, **p<0.01, ***p<0.0001).

Table I.

The table reports the main clinical data of animals included in the study, including age, gender, maximun disability score, body weigh loss and tissues destination (experiment). See text for further details

code	treatment	age (months)	gender	EAE clinical parameters		experiment
				max score	bw loss (gr)	
565	EAE	24	F	26	-21	Mol biol
572	EAE	18	F	0	-36	Mol biol
566	EAE	24	F	22	-23	IHC
571	EAE	18	M	11	-19	IHC
576	EAE	27	M	25	-38	Mol biol
573	EAE	27	F	15	-32	Mol biol
577	EAE	27	M	9	+2	IHC
582	EAE	22	F	18	-35	IHC
286	EAE	138	M	25	-3	Mol biol
342	EAE	126	F	2	-14	Mol biol
	mean+SEM	***45.1+14.5***		***15.3+3.0***	***-21.9+4.3***	
433	EAE+T3	96	F	19	-57	Mol biol
445	EAE+T3	84	M	3	-34	IHC
373	EAE+T3	96	M	0	-22	Mol biol
371	EAE+T3	96	F	5	-21	IHC
352	EAE+T3	108	M	0	-20	Mol biol
448	EAE+T3	96	F	22	-70	IHC
583	EAE+T3	24	M	18	-15	Mol biol
584	EAE+T3	24	F	7	+2	IHC
580	EAE+T3	22	F	19	-27	Mol biol
570	EAE+T3	27	M	12	+22	Mol biol
	mean+SEM	***67.3+11.8***		***10.5+2.6***	***-24.2+8.3***	
240	control	24	F			Mol biol+IHC
349	control	108	M			Mol biol+IHC
257	control	132	M			Mol biol+IHC
567	control	36	F			Mol biol+IHC
	mean+SEM	***75.0+22.5***				

Table II.

Expanded disability status scale for marmoset EAE (23). The total score is derived by adding the score for each system. The maximal score is 45. The human end-point is 25.

Function	Disability score	Maximal Score
Alertness	0: normal; 1: reduced; 2: lethargic	2
Spontaneous mobility	0: normal; 1: mild slowing; 2: marked slowing; 3: absent	3
Tremor	0: normal; 1: moderate; 2: absent	2
Tone*	0: normal; 1: mildly reduced; 2: markedly reduced; 3: absent	12
Motor (grip)*	0: normal; 1: mildly reduced; 2: markedly reduced; 3: absent	12
Sensory*		
Light Touch	0: normal; 1: reduced; 2: absent	8
Pain**	0: normal; 1: reduced; 2: absent	8**
Eye movements	0: normal; 1: abnormal	1
Vision (including pupillary reflex)	0: normal; 1: abnormal; 2: absent	2
Vocalization	0: normal; 1: changed	1
Bladder function	0: normal; 1: abnormal	1
Other signs	0: normal; 1: abnormal	1

**Scored in each limb.*
***Scored only if tactile not present.*

Table III

Thyroid hormone plasma level in the experimental groups.

	control	**EAE**	**EAE+T3**
T3, ng/ml	1.72 + 0.27	0.86 + 0.13*	1.72 + 0.14
T4, **ng/ml**	167.50 + 3.50	48.50 + 13.7*	150.40 + 3.30
rT3, ng/ml	0.12 + 0.02	0.51 + 0.14	0.36 + 0.14

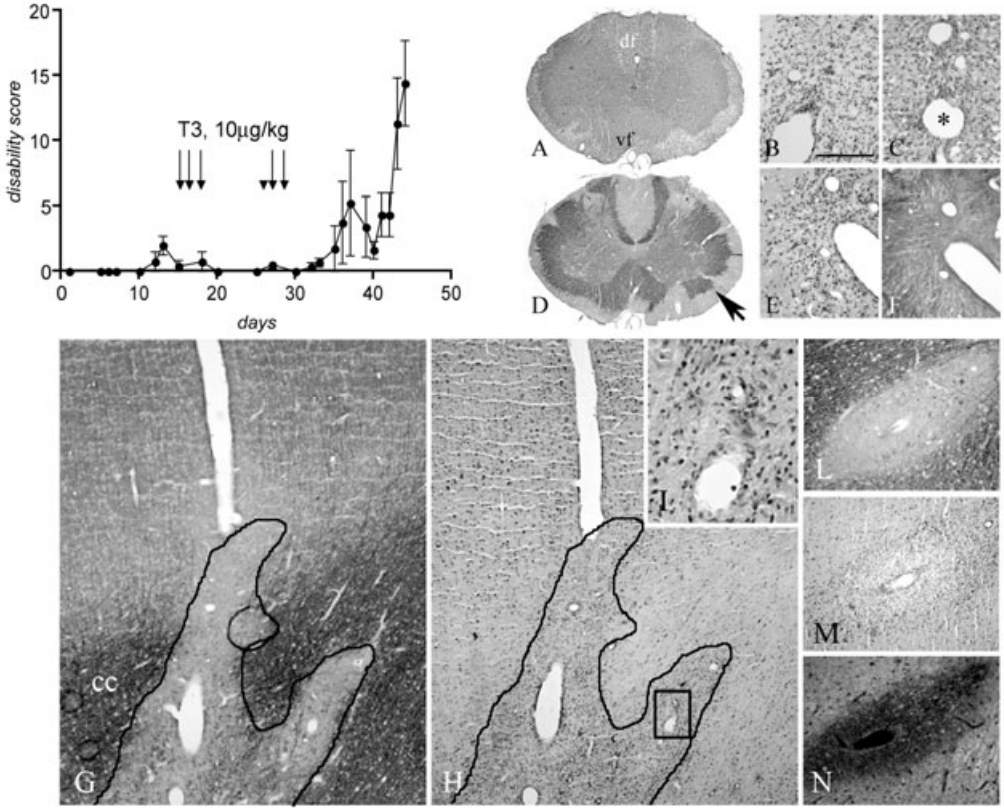
disability score
20
15
10
5
0
0
10
20
30
40
50
days
T3, 10µg/kg
df
vf
A
B
C
D
E
F
G
H
I
L
M
N
cc

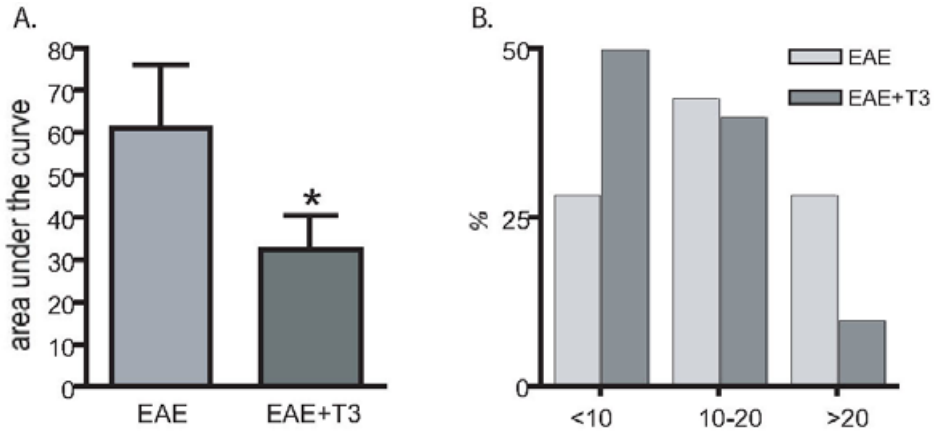
A.
area under the curve
80
70
60
50
40
30
20
10
0
*
EAE
EAE+T3
B.
50
%
25
0
EAE
EAE+T3
<10
10-20
>20

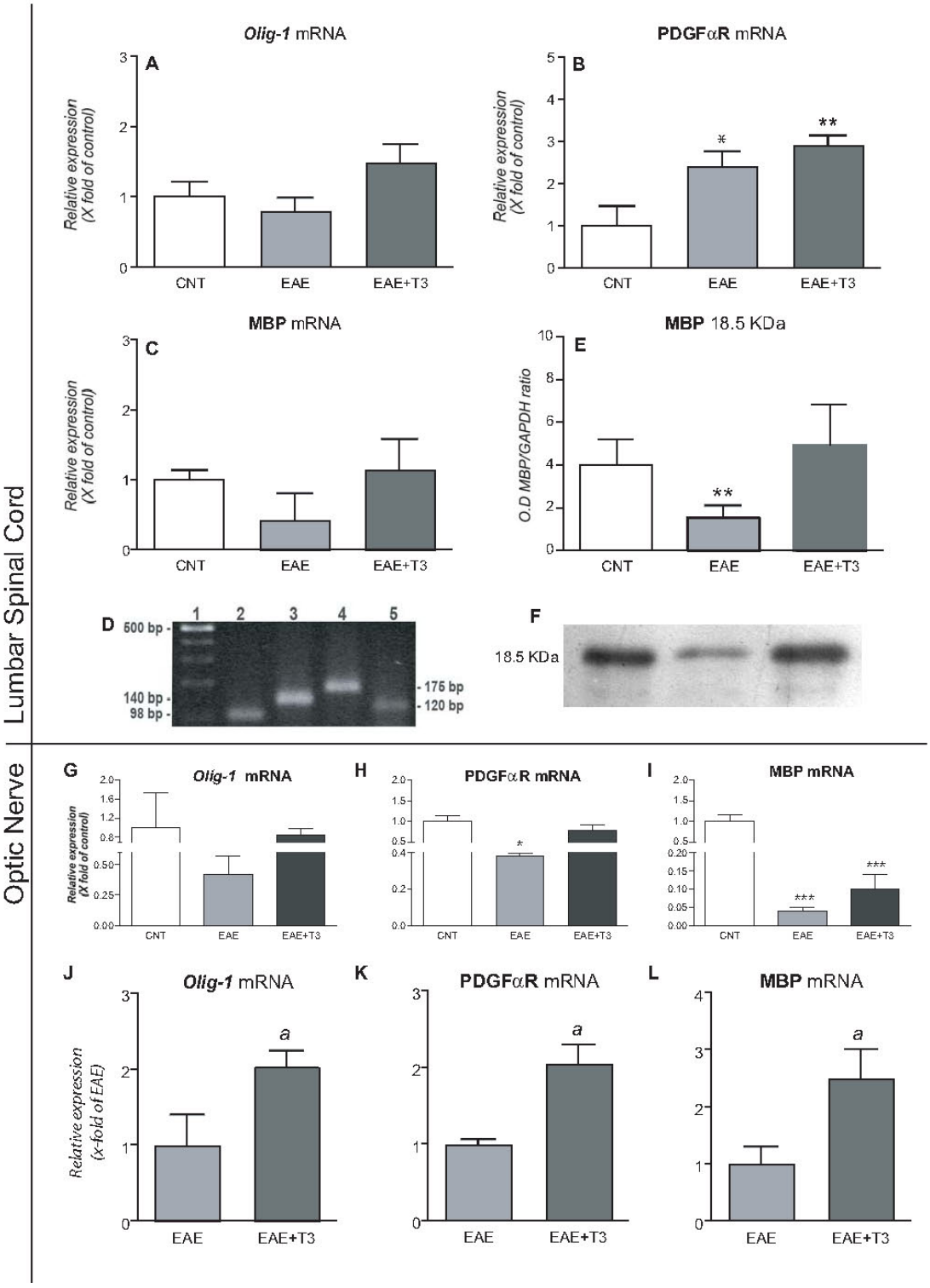
Lumbar Spinal Cord
Optic Nerve
Olig-1 mRNA
A
Relative expression (X fold of control)
CNT
EAE
EAE+T3
PDGFαR mRNA
B
*
**
MBP mRNA
C
MBP 18.5 KDa
E
O.D MBP/GAPDH ratio
D
600 bp
140 bp
98 bp
175 bp
120 bp
F
18.5 KDa
G
H
I
J
K
L
Relative expression (x-fold of EAE)
a
***

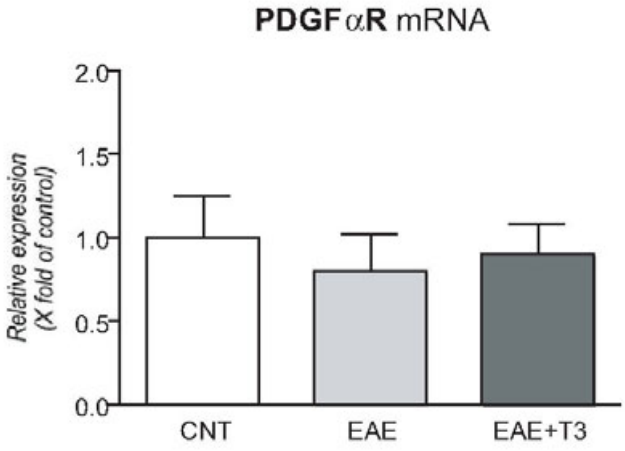
PDGFαR mRNA
Relative expression
(X fold of control)
2.0
1.5
1.0
0.5
0.0
CNT
EAE
EAE+T3

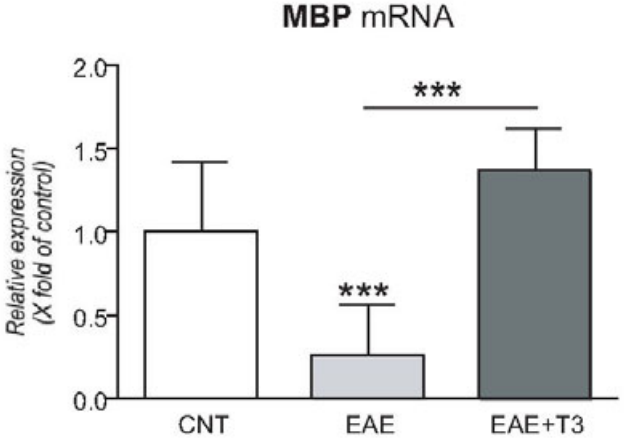
MBP mRNA
Relative expression
(X fold of control)
2.0
1.5
1.0
0.5
0.0
***
***
CNT
EAE
EAE+T3

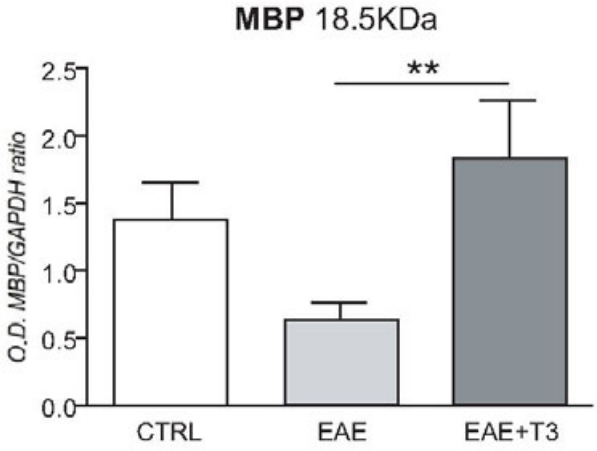
MBP 18.5KDa
O.D. MBP/GAPDH ratio
2.5
2.0
1.5
1.0
0.5
0.0
**
CTRL
EAE
EAE+T3

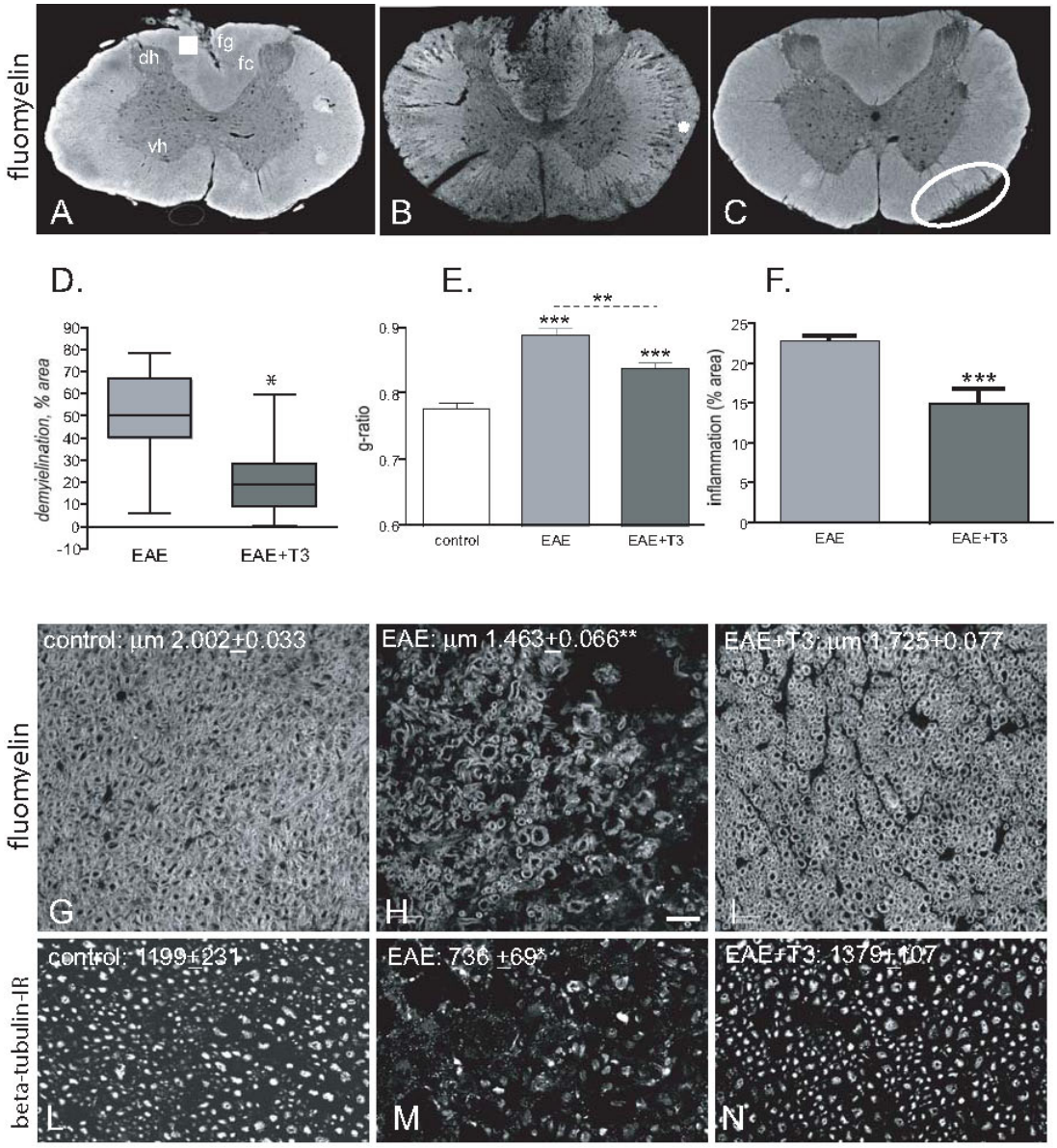
fluomyelin
dh
fg
fc
vh
A
B
C
D.
E.
F.
demyelination, % area
EAE
EAE+T3
g-ratio
control
EAE
EAE+T3
inflammation (% area)
EAE
EAE+T3
control: µm 2.002±0.033
EAE: µm 1.463±0.066**
EAE+T3: µm 1.725±0.077
G
H
I
beta-tubulin-IR
control: 1199±231
EAE: 736 ±69*
EAE+T3: 1379±107
L
M
N

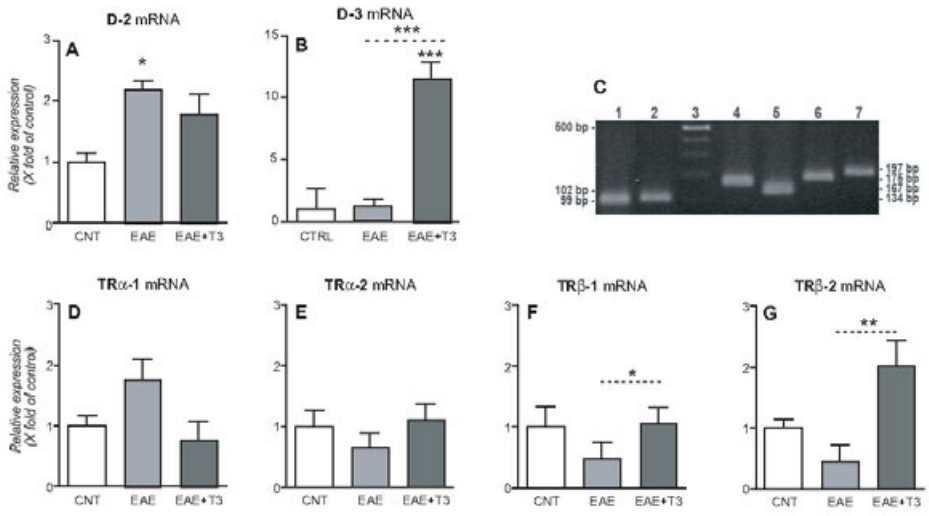
D-2 mRNA
A
*
Relative expression
(X fold of control)
CNT
EAE
EAE+T3
D-3 mRNA
B
***
***
CTRL
EAE
EAE+T3
C
1
2
3
4
5
6
7
500 bp
102 bp
99 bp
TRα-1 mRNA
D
Relative expression
(X fold of control)
CNT
EAE
EAE+T3
TRα-2 mRNA
E
CNT
EAE
EAE+T3
TRβ-1 mRNA
F
*
CNT
EAE
EAE+T3
TRβ-2 mRNA
G
**
CNT
EAE
EAE+T3